Journal of Photochemistry and Photobiology A: Chemistry 255 (2013) 27–35

Contents lists available at SciVerse ScienceDirect

Journal of Photochemistry and Photobiology A: Chemistry

journal homepage: www.elsevier.com/locate/jphotochem

New 1,3-diarylureas linked by C—C Suzuki coupling to the methyl 3-aminothieno[3,2-*b*]pyridine-2-carboxylate moiety: Synthesis and fluorescence studies in solution and in lipid membranes

Maria-João R.P. Queiroz[a,*], Daniela Peixoto[a], Ana Rita O. Rodrigues[b], Pedro M.F. Mendes[b], Cátia N.C. Costa[b], Paulo J.G. Coutinho[b], Elisabete M.S. Castanheira[b]

[a] *Departamento/Centro de Química, Universidade do Minho, Campus de Gualtar, 4710-057 Braga, Portugal*
[b] *Centro de Física (CFUM), Universidade do Minho, Campus de Gualtar, 4710-057 Braga, Portugal*

ARTICLE INFO

Article history:
Received 7 November 2012
Received in revised form 13 January 2013
Accepted 19 January 2013
Available online 28 January 2013

Keywords:
1,3-Diarylureas
Thieno[3,2-*b*]pyridines
Fluorescence
Lipid membranes
Fluorescence probes

ABSTRACT

New six fluorescent 1,3-diarylureas linked by C—C Suzuki coupling to the 6-position of the methyl 3-aminothieno[3,2-*b*]pyridine-2-carboxylate moiety were prepared by reaction of the amino groups on the *ortho* or *meta* positions relative to the C—C bond of the Suzuki coupling products, with different *para*-substituted arylisocyanates (H, OMe, CN), in high to excellent yields. The fluorescence properties of the 1,3-diarylureas in solution and in lipid membranes of egg yolk phosphatidylcholine (Egg-PC), dipalmitoyl phosphatidylcholine (DPPC), dipalmitoyl phosphatidylglycerol (DPPG) or dioctadecyldimethylammonium bromide (DODAB), with or without cholesterol (Ch), were studied. The six 1,3-diarylureas have reasonable fluorescence quantum yields in several solvents ($0.02 \leq \Phi_F \leq 0.69$) and present a moderately solvent sensitive emission, but are not fluorescent in alcohols and water. The compounds bearing the arylurea moiety in the *meta* position relative to the C—C bond, especially with the OMe and CN substituents, present the better solvatochromic properties.

Incorporation of the six compounds in lipid membranes indicates that all the compounds are deeply located in the hydrophobic region of the lipid bilayers, feeling the transition between the rigid gel phase and fluid phases.

1. Introduction

Unsymmetrical 1,3-diarylureas have attracted much attention due to their diverse applications in agriculture, medicine, petrochemicals, supramolecular chemistry (anion receptors), biology and as important intermediates and bifunctional organocatalysts in organic synthesis [1–3].

Thienopyridines including their 1,3-diarylurea derivatives have shown different biological activities, namely as antitumoral agents [4] and receptor tyrosine kinase inhibitors [5].

In this work, six new 1,3-diarylureas were prepared by reaction of aminated compounds, resulting from Suzuki coupling of methyl 3-amino-6-bromothieno[3,2-*b*]pyridine-2-carboxylate and *ortho* or *meta* pinacolborane ester anilines [6], with different *para*-substituted arylisocyanates (H, OMe, CN).

Due to the potential biological activity of the new compounds, their interaction with lipid membranes is of particular interest. The photophysical properties of these thieno[3,2-*b*]pyridine 1,3-diarylurea derivatives in solution and in lipid bilayers were studied. Lipid membranes were composed of neutral/zwitterionic phospholipids (DPPC – dipalmitoyl phosphatidylcholine; Egg-PC – egg yolk phosphatidylcholine), anionic phospholipids (DPPG – dipalmitoyl phosphatidylglycerol) or synthetic cationic lipids (DODAB – dioctadecyldimethylammonium bromide). The incorporation of cholesterol, an important component of most natural membranes, may increase the stability of the lipid aggregates by modulating the fluidity of the lipid bilayer, preventing crystallization of the phospholipid acyl chains and providing steric hindrance to their movement [7].

Fluorescence anisotropy measurements can give relevant information about the compounds behavior and location in the lipid membranes, namely if they are located deeply in the lipid bilayer, feeling the differences between the rigid gel phase and the fluid liquid-crystalline phase of the lipids.

2. Experimental

2.1. Synthesis

2.1.1. General remarks

Melting points (°C) were determined in a SMP3 Stuart apparatus and are uncorrected. ^{1}H and ^{13}C NMR spectra were recorded

* Corresponding author. Tel.: +351 253604378; fax: +351 253604382.
E-mail address: mjrpq@quimica.uminho.pt (M.-J.R.P. Queiroz).

1010-6030/$ – see front matter © 2013 Elsevier B.V. All rights reserved.
http://dx.doi.org/10.1016/j.jphotochem.2013.01.006

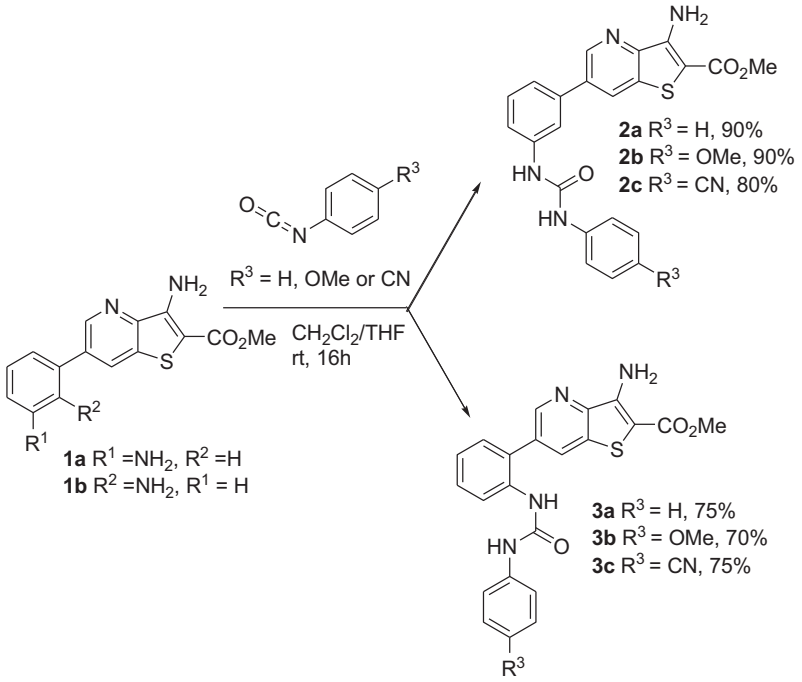

Scheme 1. Synthesis of 1,3-diarylureas **2** and **3** derivatives of thieno[3,2-*b*]pyridines by reaction of anilines with arylisocyanates.

on a Bruker Avance III at 400 and 100.6 MHz or on a Varian Unity Plus at 300 and 75.4 MHz, respectively. Heteronuclear correlations, ^{1}H–^{13}C, HMQC or HSQC were performed to attribute some signals.

HRMS data were recorded using a method of direct injection by ESI-TOF by the mass spectrometry service of the University of Vigo, Spain.

The reactions were monitored by thin layer chromatography (TLC) in aluminum plates covered with a layer of silica gel 60 (*Macherey-Nagel*) of 0.2 mm, with UV_{254} fluorescence indicator.

2.1.2. General procedure for the synthesis of 1,3-diarylureas (Scheme 1)

Compounds **1a–b** [6] and different arylisocyanates (1 equiv.) in 6 mL CH_2Cl_2:THF (1:1) were left stirring at room temperature for 16 h. If a precipitate did not come out after this time, hexane (3–5 mL) was added to the mixture to precipitate the product. This was filtered under vacuum to give the corresponding 1,3-diarylureas.

*2.1.2.1. Methyl 3-amino-6-[3-(3-phenylureido)phenyl]thieno[3,2-b]pyridine-2-carboxylate (**2a**).* From compound **1a** (80.0 mg, 0.270 mmol) and phenylisocyanate (32.0 mg) compound **2a** was isolated as a yellow solid (100 mg, 90%), m.p. 226–226.5 °C. ^{1}H NMR (400 MHz, DMSO-d_6): δ 3.83 (3H, s, OMe), 6.93 (2H, br s, NH_2), 6.95–6.99 (1H, m, ArH), 7.26–7.30 (2H, m, ArH), 7.40–7.52 (5H, m, ArH), 7.91 (1H, broad s, 2′-H), 8.62 (1H, d, J = 2 Hz, 7-H), 8.75 (1H, br s, NH), 8.82 (1H, br s, NH), 8.93 (1H, d, J = 2 Hz, 5-H) ppm. ^{13}C NMR (400 MHz, DMSO-d_6): δ 51.5 (OMe), 97.4 (C), 117.0 (2′-CH), 118.3 (2 × CH), 118.4 (CH), 121.0 (CH), 121.9 (CH), 128.8 (2× CH), 129.3 (7-CH), 129.7 (CH), 133.9 (C), 135.1 (C), 137.3 (C), 139.6 (C), 140.5 (C), 145.4 (C), 145.5 (5-CH), 147.9 (C), 152.6 (C=O), 164.6 (C=O) ppm. HRMS (ESI-TOF) Calcd. for $C_{22}H_{19}N_4O_4S$ $[M+H]^+$ 419.1172; found 419.1188.

*2.1.2.2. Methyl 3-amino-6-{3-[3-(4-methoxyphenyl)ureido]phenyl}thieno[3,2-b]pyridine-2-carboxylate (**2b**).* From compound **1a** (150 mg, 0.540 mmol) and 4-methoxyphenylisocyanate (80.0 mg) compound **2b** was isolated as a yellow solid (217 mg, 90%), m.p. 243–244 °C. ^{1}H NMR (400 MHz, DMSO-d_6): δ 3.71 (s, 3H, OMe), 3.83 (s, 3H, OMe), 6.87 (2H, d, J = 9.2 Hz, 3″ and 5″-H), 6.93 (2H, br s, NH_2), 7.36 (2H, d, J = 9.2 Hz, 2″ and 6″-H), 7.38–7.50 (3H, m, ArH), 7.89 (1H, br s, 2′-H), 8.55 (1H, br s, NH), 8.61 (1H, d, J = 2.0 Hz, 7-H), 8.73 (1H, broad s, NH), 8.92 (1H, d, J = 2.0 Hz, 5-H) ppm. ^{13}C NMR (100.6 MHz, DMSO-d_6): δ 51.6 (OMe), 55.2 (OMe), 97.4 (C), 114.0 (3″ and 5″-CH), 116.9 (2′-CH), 118.3 (CH), 120.2 (2″ and 6″-CH), 120.8 (CH), 129.3 (7-CH), 129.7 (CH), 132.6 (C), 133.9 (C), 135.2 (C), 137.3 (C), 140.7 (C), 145.4 (C), 145.5 (5-CH), 147.9 (C), 152.8 (C=O), 154.6 (C), 164.6 (C=O) ppm. HRMS (ESI-TOF) Calcd. for $C_{23}H_{21}N_4O_4S$ $[M+H]^+$ 449.1284; found 449.1284.

*2.1.2.3. Methyl 3-amino-6-{3-[3-(4-cyanophenyl)ureido]phenyl}thieno[3,2-b]pyridine-2-carboxylate (**2c**).* From compound **1a** (100 mg, 0.330 mmol) and 4-cyanophenylisocyanate (50.0 mg) compound **2c** was isolated as a yellow solid (120 mg, 80%), m.p. 264–265 °C. ^{1}H NMR (300 MHz, DMSO-d_6): δ 3.83 (3H, s, OMe), 6.94 (2H, br s, NH_2), 7.45–7.47 (2H, m, ArH), 7.49–7.54 (1H, m, ArH), 7.65 (2H, d, J = 9.0 Hz, 2″ and 6″-H), 7.73 (2H, d, J = 9.0 Hz, 3″ and 5″-H), 7.90 (1H, br s, 2′-H), 8.62 (1H, d, J = 2 Hz, 7-H), 8.92 (1H, d, J = 2.0 Hz, 5-H), 9.01 (1H, br s, NH), 9.30 (1H, br s, NH) ppm. ^{13}C NMR (75.4 MHz, DMSO-d_6): δ 51.6 (OMe), 97.4 (C), 103.4 (C), 117.4 (2′-CH), 118.1 (2″ and 6″-CH), 118.7 (CH), 119.3 (C), 121.5 (CH), 129.4 (7-CH), 129.8 (CH), 133.3 (3″ and 5″-CH), 133.9 (C), 135.0 (C), 137.4 (C), 140.0 (C), 144.1 (C), 145.5 (C), 145.6 (5-CH), 147.9 (C), 152.2 (C=O), 164.6 (C=O) ppm. HRMS (ESI-TOF) Calcd. for $C_{23}H_{18}N_5O_3S$ $[M+H]^+$ 444.1125; found 444.1120.

*2.1.2.4. Methyl 3-amino-6-[2-(3-phenylureido)phenyl]thieno[3,2-b]pyridine-2-carboxylate (**3a**).* From compound **1b** (125 mg, 0.420 mmol) and phenylisocyanate (50.0 mg) compound **3a** was isolated as a yellow solid (120 mg, 75%), m.p. 226–227 °C. ^{1}H NMR (400 MHz, DMSO-d_6): δ 3.83 (3H, s, OMe), 6.91–6.95 (m, 1H, ArH), 6.97 (2H, br s, NH_2), 7.17–7.25 (3H, m, ArH), 7.35–7.44 (4H, m, ArH), 7.86 (1H, br s, NH), 8.00 (1H, dd, J = 8.0 and 1.2 Hz, ArH), 8.43 (1H, d, J = 2 Hz, 7-H), 8.65 (1H, d, J = 2 Hz, 5-H), 8.79 (1H, br s, NH) ppm. ^{13}C NMR (100.6 MHz, DMSO-d_6): δ 51.6 (OMe), 97.3 (C), 118.0 (2× CH), 121.8 (CH), 122.6 (CH), 123.5 (CH), 128.8 (2× CH), 128.9 (CH), 129.1 (C), 130.7 (CH), 132.1 (7-CH), 133.7 (C), 133.8 (C), 136.5 (C), 139.6 (C), 145.3 (C), 147.3 (5-CH), 148.0 (C), 152.6

(C=O), 164.6 (C=O) ppm. HRMS (ESI-TOF) Calcd. for $C_{22}H_{19}N_4O_3S$ $[M+H]^+$ 419.1172; found 419.1180.

*2.1.2.5. Methyl 3-amino-6-{2-[3-(4-methoxyphenyl)ureido]phenyl} thieno[3,2-b]pyridine-2-carboxylate (**3b**).* From compound **1b** (100 mg, 0.330 mmol) with 4-methoxyphenylisocyanate (50.0 mg) compound **3b** was obtained (100 mg, 70%), m.p. 243–244 °C. ^{1}H NMR (400 MHz, DMSO-d_6): δ 3.68 (3H, s, OMe), 3.83 (3H, s, OMe), 6.81 (2H, d, J = 9.2 Hz, 3″ and 5″-H), 6.97 (2H, br s, NH_2), 7.15–7.19 (1H, m, ArH), 7.25 (2H, d, J = 9.2 Hz, 2″ and 6″-H), 7.32–7.35 (1H, m, ArH), 7.38–7.42 (1H, m, ArH), 7.77 (1H, br s, NH), 7.99 (1H, br d, J = 8.4 Hz, ArH), 8.42 (1H, d, J = 2.0 Hz, 7-H), 8.63 (1H, br s, NH), 8.64 (1H, d, J = 2.0 Hz, 5-H). ^{13}C (100.6 MHz, DMSO-d_6): δ 51.6 (OMe), 55.1 (OMe), 97.2 (C), 114.0 (3″ and 5″-CH), 119.8 (2″ and 6″-CH), 122.3 (CH), 123.2 (CH), 128.9 (CH), 130.7 (CH), 132.1 (7-CH), 132.6 (C), 133.8 (C), 136.7 (C), 145.3 (C), 147.3 (5-CH), 148.0 (C), 152.7 (C=O), 154.4 (C), 164.6 (C=O) ppm. HRMS (ESI-TOF) Calcd. for $C_{23}H_{21}N_4O_4S$ $[M+H]^+$ 449.1284; found 449.1280.

*2.1.2.6. Methyl 3-amino-6-{2-[3-(4-cyanophenyl)ureido]phenyl} thieno[3,2-b]pyridine-2-carboxylate (**3c**).* From compound **1b** (140 mg, 0.470 mmol) and 4-cyanophenylisocyanate (69.0 mg) compound **3c** was isolated as a yellow solid (120 mg, 75%), m.p. 210–211 °C. ^{1}H NMR (400 MHz, DMSO-d_6): δ 3.83 (3H, s, OMe), 6.96 (2H, br s, NH_2), 7.22–7.26 (1H, m, ArH), 7.36–7.39 (1H, m, ArH), 7.52–7.55 (1H, m, ArH), 7.53 (2H, d, J = 8.8 Hz, 2″ and 6″-H), 7.67 (2H, d, J = 8.8 Hz, 3″ and 5″-H), 7.93–7.95 (1H, m, ArH), 8.07 (1H, br s, NH), 8.44 (1H, d, J = 2 Hz, 7-H), 8.65 (1H, d, J = 2.0 Hz, 5-H), 9.28 (1H, br s, NH) ppm. ^{13}C NMR (100.6 MHz, DMSO-d_6): δ 51.6 (OMe), 97.3 (C), 103.3 (C), 117.9 (2″ and 6″-CH), 119.3 (C), 123.2 (CH), 124.2 (CH), 129.0 (CH), 129.8 (C), 130.8 (CH), 132.1 (7-CH), 133.3 (3″ and 5″-CH), 133.6 (C), 133.7 (C), 135.8 (C), 144.1 (C), 145.3 (C), 147.2 (5-CH), 147.9 (C), 152.3 (C=O), 164.6 (C=O) ppm. HRMS (ESI-TOF) Calcd. for $C_{23}H_{18}N_5O_3S$ $[M+H]^+$ 444.1125; found 444.1129.

2.2. Lipid membranes preparation

All the solutions were prepared using spectroscopic grade solvents and ultrapure water (Milli-Q grade). 1,2-Dipalmitoyl-*sn*-glycero-3-phosphocholine (DPPC), 1,2-diacyl-*sn*-glycero-3-phosphocholine from egg yolk (Egg-PC), 1,2-dipalmitoyl-*sn*-glycero-3-[phospho-*rac*-(1-glycerol)] (sodium salt) (DPPG) and cholesterol were obtained from Sigma–Aldrich and dioctadecyldimethylammonium bromide (DODAB) from Tokyo Kasei (lipid structures are shown below).

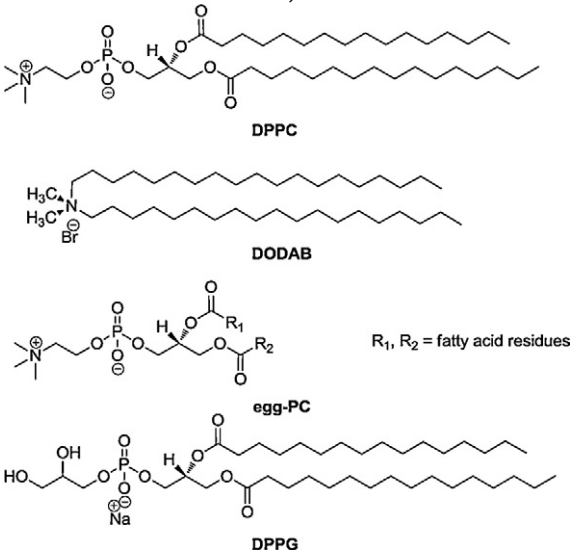

For lipid vesicles preparation, the ethanolic injection method was used [8–10]. For Egg-PC membranes preparation, defined volume of stock solution of lipid (86.2 mM) and each compound (0.3 mM) in ethanol were injected together, under vigorous stirring, to an aqueous buffer solution (10 mM Tris, pH = 7.4), at room temperature. A similar procedure was adopted for DPPC, DODAB and DPPG vesicles, but the injection of the required amounts of stock solutions of lipid (50 mM for DPPC, 20 mM for DODAB and 26.8 mM for DPPG) and compounds in ethanol was done at 60 °C, well above the melting transition temperature of each lipid (*ca.* 41 °C for DPPC [11], *ca.* 45 °C for DODAB [12], and 39.6 °C for DPPG [13]). In all cases, the final lipid concentration was 1 mM, with a compound/lipid molar ratio of 1:333.

2.3. Spectroscopic measurements

Absorption spectra were recorded in a Shimadzu UV-3101PC UV–vis–NIR spectrophotometer. Fluorescence measurements were performed using a Fluorolog 3 spectrofluorimeter, equipped with double monochromators in both excitation and emission, Glan-Thompson polarizers and a temperature controlled cuvette holder. Fluorescence spectra were corrected for the instrumental response of the system.

For fluorescence quantum yield determination, the solutions were previously bubbled for 20 min with ultrapure nitrogen. The fluorescence quantum yields (Φ_s) were determined using the standard method (Eq. (1)) [14,15]. Quinine sulfate in H_2SO_4 0.05 M was used as reference, Φ_r = 0.546 at 25 °C [16].

$$\Phi_s = \left[\frac{A_r F_s n_s^2}{A_s F_r n_r^2}\right] \Phi_r \quad (1)$$

where A is the absorbance at the excitation wavelength, F is the integrated emission area and n is the refraction index of the solvents used. Subscripts refer to the reference (r) or sample (s) compound. The absorbance value at excitation wavelength was always less than 0.1, in order to avoid inner filter effects.

Solvatochromic shifts can be described by the Lippert–Mataga equation (2), which relates the energy difference between absorption and emission maxima to the orientation polarizability [17,18]

$$\overline{\nu}_{abs} - \overline{\nu}_{fl} = \frac{1}{4\pi\varepsilon_0}\frac{2\Delta\mu^2}{hcR^3}\Delta f + \text{const} \quad (2)$$

where $\overline{\nu}_{abs}$ is the wavenumber of maximum absorption, $\overline{\nu}_{fl}$ is the wavenumber of maximum emission, $\Delta\mu = \mu_e - \mu_g$ is the difference in the dipole moment of solute molecule between excited (μ_e) and ground (μ_g) states, R is the cavity radius (considering the fluorophore a point dipole at the center of a spherical cavity immersed in the homogeneous solvent), and Δf is the orientation polarizability given by (Eq. (3)):

$$\Delta f = \frac{\varepsilon - 1}{2\varepsilon + 1} - \frac{n^2 - 1}{2n^2 + 1} \quad (3)$$

where ε is the static dielectric constant and n is the refractive index of the solvent.

An alternative expression, proposed by Bakhshiev, takes into account the angle, γ, between the ground and excited state dipole moments of the fluorophore [19,20]:

$$\overline{\nu}_{abs} - \overline{\nu}_{fl} = \frac{1}{4\pi\varepsilon_0}\frac{2}{hcR^3}(\mu_g^2 - 2\mu_g\mu_e\cos\gamma + \mu_e^2)f(\varepsilon, n) + \text{const} \quad (4)$$

where $\mu_g^2 - 2\mu_g\mu_e\cos\gamma + \mu_e^2$ is equivalent to $|\vec{\mu}_e - \vec{\mu}_g|^2$ and

$$f(\varepsilon, n) = \frac{\varepsilon - 1}{\varepsilon + 2} - \frac{n^2 - 1}{n^2 + 2} \quad (5)$$

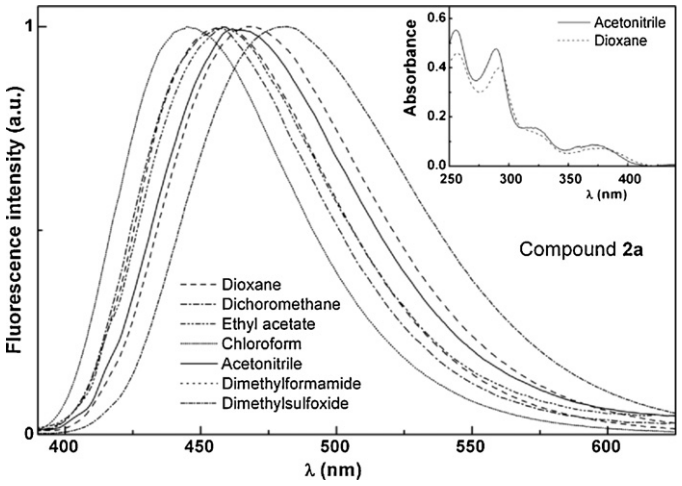

Fig. 1. Normalized fluorescence spectra of 3×10^{-6} M solutions of compound **2a** in several solvents (λ_{exc} = 370 nm). Inset: absorption spectrum of 10^{-5} M solutions of **2a** in dioxane and acetonitrile, as examples.

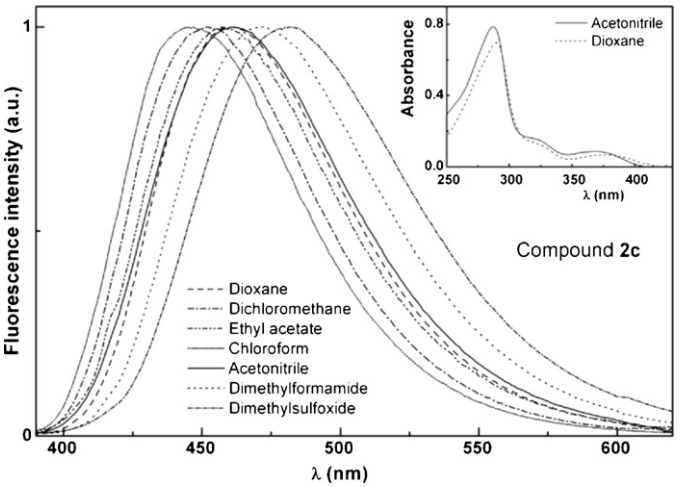

Fig. 2. Normalized fluorescence spectra of 3×10^{-6} M solutions of compound **2c** in several solvents (λ_{exc} = 370 nm). Inset: absorption spectrum of 10^{-5} M solutions of **2c** in dioxane and acetonitrile, as examples.

The steady-state fluorescence anisotropy, r, is calculated by

$$r = \frac{I_{VV} - GI_{VH}}{I_{VV} + 2GI_{VH}} \quad (6)$$

where I_{VV} and I_{VH} are the intensities of the emission spectra obtained with vertical and horizontal polarization, respectively (for vertically polarized excitation light), and $G = I_{HV}/I_{HH}$ is the instrument correction factor, where I_{HV} and I_{HH} are the emission intensities obtained with vertical and horizontal polarization (for horizontally polarized excitation light).

3. Results and discussion

3.1. Synthesis

New 1,3-diarylureas **2a–c** and **3a–c** were prepared by reaction of the aromatic amino groups of the Suzuki coupling products **1a–b**, earlier obtained by us from methyl 3-amino-6-bromothieno[3,2-*b*]pyridine-2-carboxylate and pinacolborane esters of anilines [6], with arylisocyanates, in high to excellent yields (Scheme 1).

3.2. Fluorescence studies in several solvents

The absorption and fluorescence properties of compounds **2a–c** and **3a–c** were studied in several solvents (Table SD1 in Supplementary Data). The normalized fluorescence spectra of compounds **2a**, **2c** and **3b** are shown in Figs. 1–3, respectively (examples of absorption spectra are also shown as insets).

Supplementary material related to this article found, in the online version, at http://dx.doi.org/10.1016/j.jphotochem.2013.01.006.

Compounds **2a–c** and **3a–c** exhibit reasonable fluorescence emission in several solvents (the studied solvents do not include cyclo- or *n*-alkanes, because the solubility of these compounds is very poor in this kind of solvents). Fluorescence quantum yield values are in the range of 6% in chloroform and 65% in DMSO for compounds **2a–c** and of 2% (chloroform) and 69% (DMSO) for compounds **3a–c** (Table SD1). However, no emission is observed in protic solvents like water, methanol or ethanol.

This behavior, already observed for di(hetero)arylether derivatives of thieno[3,2-*b*]pyridines recently synthesized [21], can be due to specific solute–solvent interactions by hydrogen bonds with protic solvents, namely by protonation of the nitrogen atom of the pyridine ring. The same explanation can justify the low fluorescence quantum yields obtained in chloroform, as the formation of hydrogen bonds between chloroform and proton acceptor molecules has been already described [22].

The six compounds studied here are more fluorescent in polar solvents like dimethylformamide and dimethylsulfoxide, which is also a common behavior with the di(hetero)arylether derivatives of thieno[3,2-*b*]pyridines studied earlier [21]. Also, the substituent does not seem to have a significant influence in the fluorescence quantum yield values (Table SD1).

For all compounds, significant red shifts are observed for emission in polar solvents (34–36 nm between chloroform and dimethylsulfoxide for compounds **2a–c** and 20–25 nm for **3a–c**). In the absorption spectra, the red shifts are negligible (Table SD1), indicating that solvent relaxation after photoexcitation plays an important role, especially for compounds **2a–c**. This indicates that the 1,3-arylurea substituent in the *meta* position relative to C—C bond contributes to increase the intramolecular charge transfer (ICT) character of the excited state.

The solvatochromic plots for compounds **2a–c** and **3a–c**, shown in Figs. 4 and 5, are reasonably linear, the slope being larger for compound **2c**. This predicts a higher ICT character of the excited

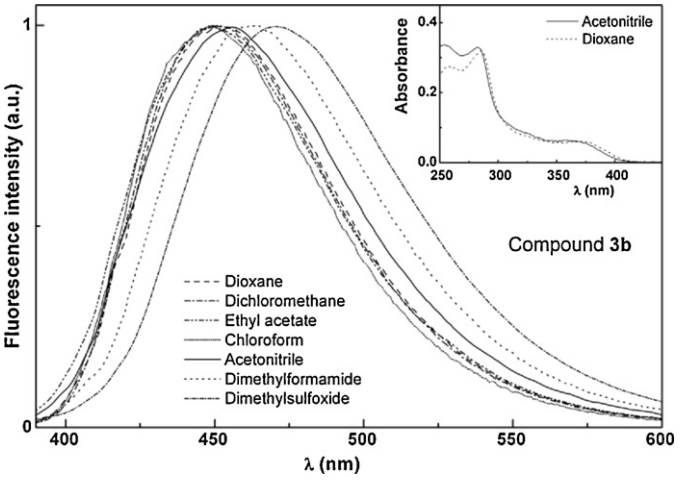

Fig. 3. Normalized fluorescence spectra of 3×10^{-6} M solutions of compound **3b** in several solvents (λ_{exc} = 370 nm). Inset: absorption spectrum of 10^{-5} M solutions of **3b** in dioxane and acetonitrile, as examples.

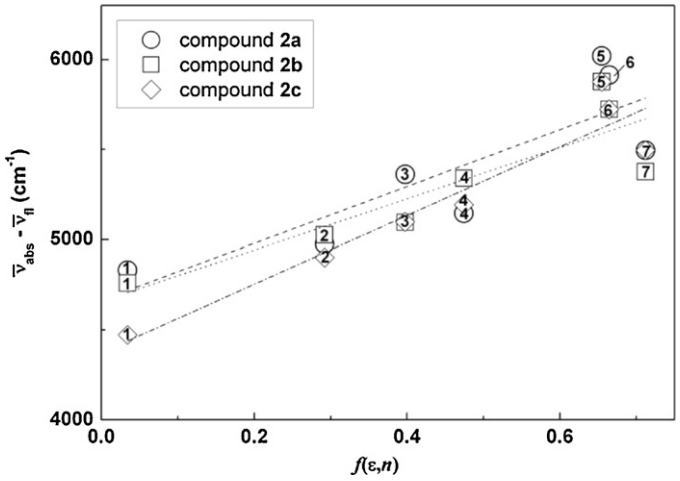

Fig. 4. Solvatochromic plots (Eq. (4)) for compounds **2a–c**. Solvents: 1 – dioxane; 2 – chloroform; 3 – ethyl acetate; 4 – dichloromethane; 5 – dimethylsulfoxide; 6 – *N*,*N*-dimethylformamide; 7 – acetonitrile (values of ε and n were obtained from Ref. [23]).

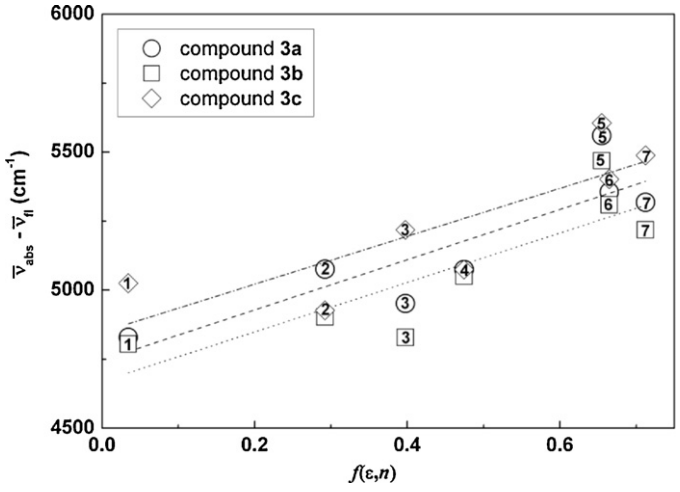

Fig. 5. Solvatochromic plots (Eq. (4)) for compounds **3a–c**. Solvents: 1 – dioxane; 2 – chloroform; 3 – ethyl acetate; 4 – dichloromethane; 5 – dimethylsulfoxide; 6 – *N*,*N*-dimethylformamide; 7 – acetonitrile (values of ε and n were obtained from Ref. [23]).

state for this compound, maybe related with the position of the arylurea moiety together with the presence of a nitrile substituent.

The slopes of the solvatochromic plots are much lower for compounds **3a–c**, being similar for these three molecules. This indicates that the charge transfer character of the excited state is much lower for the arylureas in the *ortho* position relative to the thieno[3,2-*b*]pyridine-2-carboxylate moiety.

From *ab initio* molecular quantum chemistry calculations, obtained with Gaussian 09 software [24] and use of a 6-311+G(dp) basis set at the DFT (CAM-B3LYP/AUTO) level of theory [24,25] in gas phase, the cavity radius (R) and the ground state dipole moment (μ_g) were determined for the six compounds (Table 2). The use of CAM-B3LYP functional was needed, as initial trials with the simpler B3LYP gave unrealistic underestimates of the HOMO–LUMO band gap (<500 nm). This is a known problem with B3LYP functional in the description of excited states with charge transfer character [25]. The optimized geometries of the ground state and the first excited state were obtained with a smaller basis set (3-21G+*) and are similar in the groups of compounds **2a–c** and **3a–c** (Figs. 6 and 7). In the case of excited state calculations, a time dependent density functional method was used (TD-SCF DFT). In Table 1, the dihedral angle defined by the two molecular planes and the angles for the N—C—N and C—S—C chemical bonds (in the thienopyridine moiety) are indicated, evidencing notable differences in geometries between the two sets of compounds. Comparing the ground and excited state geometries, a small decrease (*ca.* 10° in **2a–c** and 5° in **3a–c**) of the dihedral angle is observed in the excited state (Table 1), together with a 2° increase in the C—S—C bond angle for all compounds.

Table 1
Dihedral angle α, N—C—N bond angle β and C—S—C bond angle γ in the ground and first singlet excited state geometries for compounds **2a–c** and **3a–c**.

Compound	State	Dihedral angle α	N—C—N angle β	C—S—C angle γ
2a	Ground	−46.6°	112.6°	90.1°
	Excited	−36.8°	112.8°	92.6°
2b	Ground	−46.9°	112.5°	90.1°
	Excited	−36.6°	112.8°	92.6°
2c	Ground	−47.0°	112.5°	90.1°
	Excited	−36.1°	112.7°	92.6°
3a	Ground	94.0°	112.3°	90.1°
	Excited	89.6°	112.5°	92.7°
3b	Ground	94.7°	112.2°	90.1°
	Excited	89.0°	112.5°	92.8°
3c	Ground	94.0°	112.2°	90.1°
	Excited	89.8°	112.4°	92.7°

The directions of the calculated dipole moments in the ground and excited states are also indicated in Figs. 6 and 7, evidencing an increase in magnitude and a change of direction in the excited state dipole moment vector relative to the ground state one. This clearly indicates that the angle between the two dipole moment vectors cannot be neglected and must be considered in the solvatochromic plots (Bakhshiev's equation (4)). Nevertheless, the change in the dipole moment direction is very small for compounds **2c** and **3a**. In the excited state, the dipole moment vectors for all compounds point to the side of the thienopyridine moiety.

The absolute value of the difference in the excited and ground state dipole moment vectors, estimated from the solvatochromic plots (Figs. 4 and 5) and from molecular quantum mechanical calculations, is presented in Table 2, for each compound. The obtained values are very similar and, therefore, both methods point to the presence of a charge transfer mechanism in the excited state, more pronounced for compounds **2a–c**. Compounds bearing an

Table 2
Cavity radius (R), ground (μ_g) and excited state (μ_e) dipole moments obtained from theoretical calculations, and absolute value of the dipole moment difference ($|\vec{\mu}_e - \vec{\mu}_g|$), from quantum mechanical calculations and from the solvatochromic plots.

Compound	Cavity radius, R (Å)	Ground state dipole moment, μ_g (D)	Excited state dipole moment, μ_e (D), from theoretical calculations	$\lvert\vec{\mu}_e - \vec{\mu}_g\rvert$ (D) from theoretical calculations	$\lvert\vec{\mu}_e - \vec{\mu}_g\rvert$ (D) from solvatochromic plots
2a	5.6	3.1	6.1	5.1	5.2
2b	6.2	4.7	7.3	5.2	5.8
2c	5.9	4.9	10.1	5.3	6.2
3a	5.7	2.2	6.7	4.6	4.1
3b	6.0	3.3	7.8	4.5	4.4
3c	5.9	7.4	10.2	4.7	4.2

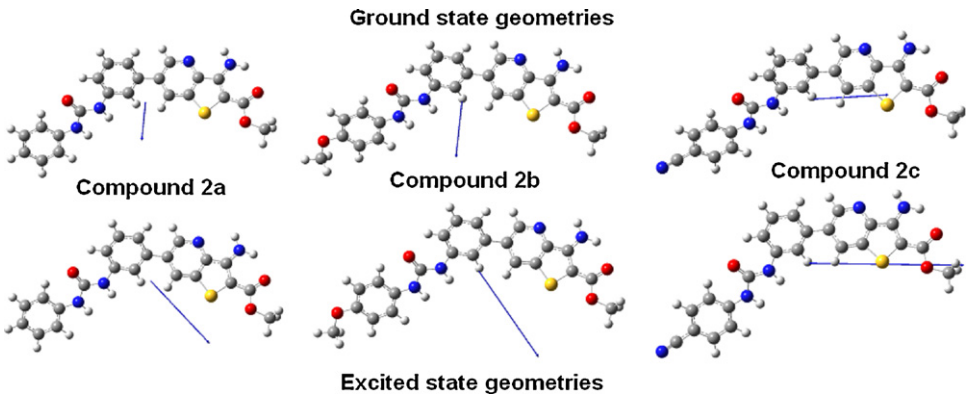

Fig. 6. Optimized geometries of compounds **2a–c** obtained by Gaussian 09 software (gray: C atoms; white: H atoms; red: O atoms; blue: N atoms; yellow: S atoms). Above: ground state; below: lowest excited singlet state. The arrows indicate the direction of the dipole moment. (For interpretation of the references to color in this figure legend, the reader is referred to the web version of the article.)

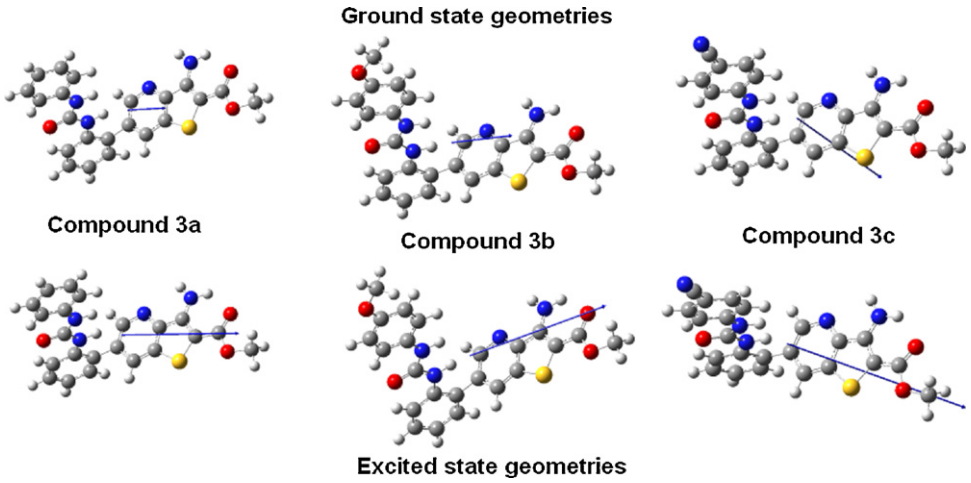

Fig. 7. Optimized geometries of compounds **3a–c** obtained by Gaussian 09 software (gray: C atoms; white: H atoms; red: O atoms; blue: N atoms; yellow: S atoms). Above: ground state; below: lowest excited singlet state. The arrows indicate the direction of the dipole moment. (For interpretation of the references to color in this figure legend, the reader is referred to the web version of the article.)

electron-donating group (—OCH_3 in **2b)** or an electron-withdrawing group (—CN in **2c**) have a higher ICT character of the excited state than compound **2a**.

Fig. 8 displays the representation of electronic density difference between the lowest excited state and the ground state, for the lowest excited state optimized geometry (relaxed S_1 state). In general, it can be observed that electron density variations reside mostly on the thienopyridine-2-carboxylate moiety. This justifies that the compounds do not exhibit a noticeable influence of the arylurea substituent (—OCH_3 or —CN) in their photophysical properties, namely in the fluorescence quantum yields. The more prominent features in Fig. 8 are an electron density transfer from the amino

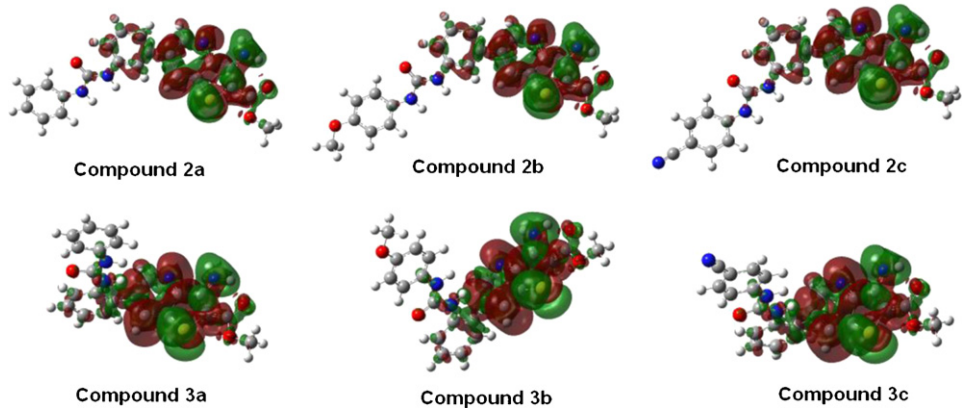

Fig. 8. Representation of the electronic density difference for compounds **2a–c** and **3a–c** (optimized geometry for the lowest excited singlet state) at an iso level of 0.0004; green regions: loss of electronic density; red regions: enrichment of electronic density. (For interpretation of the references to color in this figure legend, the reader is referred to the web version of the article.)

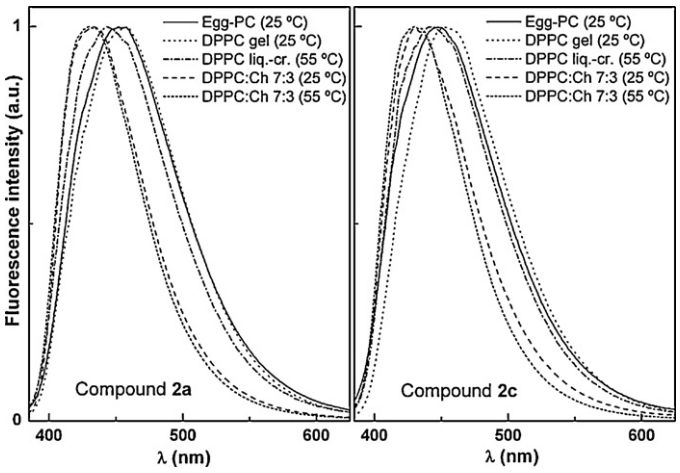

Fig. 9. Normalized fluorescence spectra of compounds **2a** and **2c** (3×10^{-6} M) in lipid aggregates of Egg-PC, Egg-PC:Ch, DPPC and DPPC:Ch, at 25 °C and 55 °C.

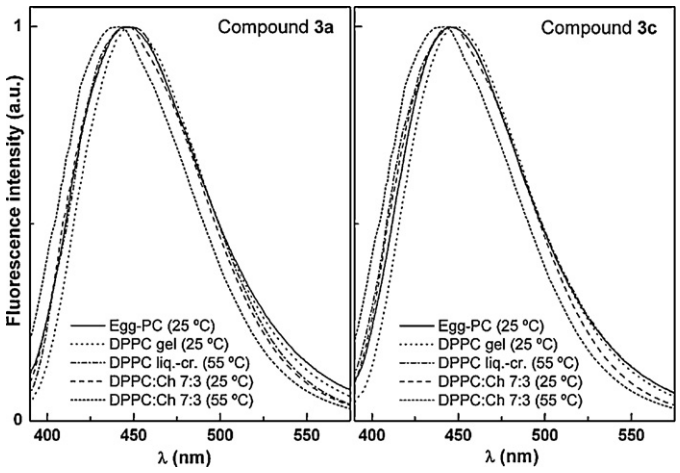

Fig. 10. Normalized fluorescence spectra of compounds **3a** and **3c** (3×10^{-6} M) in lipid aggregates of Egg-PC, Egg-PC:Ch, DPPC and DPPC:Ch, at 25 °C and 55 °C.

group linked to the thiophene ring and its sulfur atom to the nitrogen atom in the pyridine moiety and to the carboxylate group. In the π-electron system, alternating increases and decreases of electronic density are observed. This confirms the ICT character of the first excited state of these compounds.

The photophysical behavior of the six compounds shows that they can be considered as solvatochromic probes, especially compounds **2a**–**c**. The sensitivity of the fluorescence emission to the fluorophore environment can be very useful when probing the location/behavior of these compounds in lipid membranes.

3.3. Fluorescence studies in lipid membranes

Fluorescence experiments of the six compounds incorporated in lipid membranes of several compositions were carried out. These lipid aggregates were composed either by neat phospholipids, or by phosphatidylcholines with cholesterol (Ch), for a better simulation of the biological membranes. In fact, the vesicles composed of 70% Egg-PC and 30% cholesterol (Egg-PC:Ch (7:3)) are often used as models of the biological membranes [26,27].

Lipid membranes of neat DPPC (zwitterionic), DPPG (anionic), DODAB (cationic), Egg-PC (zwitterionic, composed of a phosphatidylcholine mixture), Egg-PC:Ch (7:3) and DPPC:Ch (7:3), with incorporated compounds, were prepared and the fluorescence emission was monitored in both gel (below the main transition temperature, T_m) and liquid-crystalline (above T_m) phases of the phospholipids. At room temperature, the phospholipids DPPC, DODAB and DPPG are in ordered gel phase, where the hydrocarbon chains are fully extended and closely packed. The melting transition temperature of Egg-PC is very low [28] and this lipid is in the fluid liquid-crystalline phase at room temperature.

Fluorescence spectra of compounds incorporated in these lipid aggregates are presented in Figs. 9 and 10. All the six compounds exhibit reasonable fluorescence emission when incorporated in lipid membranes, indicating that they are mainly located in the region of the lipid bilayer, as they are not fluorescent in alcohols or water. The maximum emission wavelengths in lipid membranes generally point to a hydrophobic medium for all compounds in these lipid aggregates, feeling an environment with polarity near dioxane or less polar than dioxane (Table 3). A slightly more hydrated environment is anticipated for the six compounds in DPPG vesicles at 25 °C, considering the values of the maximum emission wavelengths.

Fluorescence anisotropy (r) measurements can give relevant information about the location of the compounds in liposomes, as r increases with the rotational correlation time of the fluorescent molecule (and, thus, with the viscosity of the fluorophore environment) [29].

Steady-state anisotropy relates to both the excited-state lifetime and the rotational correlation time of the fluorophore [29],

$$\frac{1}{r} = \frac{1}{r_0}\left(1 + \frac{\tau}{\tau_c}\right) \quad (7)$$

where r_0 is the fundamental anisotropy, τ is the excited-state lifetime and τ_c is the rotational correlation time.

The fluorescence steady-state anisotropies of compounds **2a**–**c** and **3a**–**c** in lipid membranes are shown in Table 3. Anisotropy values in glycerol at room temperature were also determined for comparison.

Steady-state fluorescence anisotropy results (Table 3) allow concluding that all compounds are mainly located in the inner region of the lipid membrane. The transition from the rigid gel phase to the fluid liquid-crystalline phase is clearly detected by a notable decrease in anisotropy at 55 °C. An increase of the steady-state anisotropy is predicted from a decrease of the excited-state lifetime (Eq. (7)). Upon rising temperature (from 25 °C to 55 °C), the excited-state lifetime decreases due to the increase of non-radiative deactivation pathways (mainly the rate constant for internal conversion $S_1 \rightarrow S_0$). Instead of an expected rise in anisotropy (Eq. (7)), a decrease is observed, which can only be attributed to a diminution of the rotational correlation time of the fluorophore, that arises from the decrease of membrane microviscosity upon changing from the gel to the liquid-crystalline phase.

Fluorescence anisotropy values for the compounds incorporated in lipid membranes exhibit also a significant decrease when lipid aggregate fluidity increases by addition of cholesterol. Simultaneously, a blue shift in emission spectra (Figs. 9 and 10 and Table 3) is observed when fluidity increases, either by phase transition to the liquid-crystalline phase or by cholesterol addition. These changes are much more pronounced for compounds **2a**–**c** and may indicate a relocation of the fluorophores in a less hydrated environment. The decrease in local microviscosity can facilitate a deeper penetration of these molecules in lipid bilayers. The results obtained here point to a promising utility of the new diarylureas to monitor changes in fluidity of lipid membranes, especially compounds **2a**–**c**.

Microviscosity in hydrophobic domains of microheterogeneous systems has been measured using the widely known fluorescence probe 1,3-bis-(1-pyrenyl)propane (BPP) [30–35]. This probe can form intramolecular excimers and is highly sensitive to constraints imposed by its environment, reported by variations in the ratio

Table 3
Steady-state fluorescence anisotropy (r) values and maximum emission wavelengths (λ_{em}) for compounds **2a–c** and **3a–c** in lipid aggregates, below (25 °C) and above (55 °C) transition temperature of the lipids. Anisotropy values in glycerol at room temperature are also shown for comparison.

Lipid	T (°C)	**2a**		**2b**		**2c**		**3a**		**3b**		**3c**	
		λ_{em} (nm)	r	λ_{em} (nm)	r	λ_{em} (nm)	r	λ_{em} (nm)	r	λ_{em} (nm)	r	λ_{em} (nm)	r
Egg-PC	25	452	0.221	449	0.205	451	0.210	449	0.248	451	0.249	449	0.240
Egg-PC:Ch (7:3)	25	443	0.197	440	0.187	443	0.190	446	0.228	446	0.221	445	0.231
DPPC	25	458	0.238	459	0.232	452	0.262	452	0.256	451	0.259	452	0.251
	55	443	0.168	441	0.167	443	0.175	449	0.163	448	0.122	449	0.180
DPPC:Ch (7:3)	25	434	0.172	438	0.175	439	0.192	450	0.199	449	0.171	450	0.194
	55	430	0.143	432	0.136	431	0.155	446	0.104	445	0.118	446	0.127
DODAB	25	457	0.229	457	0.200	453	0.243	448	0.230	456	0.251	451	0.247
	55	446	0.182	447	0.167	446	0.131	445	0.172	444	0.180	444	0.183
DPPG	25	467	0.230	466	0.223	466	0.250	461	0.233	464	0.226	457	0.209
	55	457	0.181	458	0.190	457	0.195	457	0.149	460	0.138	454	0.102
Glycerol	25	474	0.325	465	0.295	469	0.308	464	0.330	462	0.327	459	0.324

between excimer and monomer emission intensities. The new diarylurea derivatives **2a–c** and **3a–c** showed in this work an interesting potential as fluidity probes for lipid membranes (especially **2a–c**) through their intrinsic photophysical properties, rather than by the relative efficiency of a dynamic conformational change leading to an intramolecular pyrene excimer formation, as observed in BPP. However, further studies are needed to assess the utility of these new probes for microviscosity determinations of other types of microheterogeneous systems already studied using BPP, like micelles, liquid crystals, lipoproteins and synthetic polymers [30,33–35].

4. Conclusions

New six fluorescent 1,3-diarylureas in the thieno[3,2-*b*]pyridine series were prepared by a reaction of *ortho* and *meta* aminated Suzuki coupling products obtained by the formation of a C—C bond in the 6-position of the thieno[3,2-*b*]pyridine moiety, with different *para*-substituted arylisocyanates (H, OMe or CN).

The six compounds exhibit reasonable fluorescence quantum yields in several solvents and present a moderately solvent sensitive emission, but are not fluorescent in alcohols and water. Compounds **2b** and **2c** with the arylurea moiety in the *meta* position and bearing a OMe or CN group, are the ones with better solvatochromic properties.

Incorporation of compounds **2a–c** and **3a–c** in lipid membranes indicate that all compounds are deeply located in the hydrophobic region of the lipid bilayers, feeling the transition between the rigid gel phase and the liquid-crystalline phase. The results obtained point to a promising utility of these compounds to monitor changes in fluidity of lipid membranes, especially compounds **2a–c**. Moreover, due to the potential biological activity of these new compounds, their interaction with lipid membranes is of particular interest.

Acknowledgements

To the Foundation for the Science and Technology (FCT, Portugal) for financial support to the NMR Portuguese network (PTNMR, Bruker Avance III 400-Univ. Minho). To the FCT and FEDER (European Fund for Regional Development)-COMPETE-QREN-EU for financial support to the Research Centres, CQ/UM [PEst-C/QUI/UI0686/2011 (FCOMP-01-0124-FEDER-022716)] and CFUM [PEst-C/FIS/UI0607/2011 (F-COMP-01-0124-FEDER-022711)], and to the research projects PTDC/QUI/81238/2006 (FCOMP-01-0124-FEDER-007467) (photophysical studies) and PTDC/QUI-QUI/111060/2009 (F-COMP-01-0124-FEDER-015603) (organic synthesis).

References

[1] V. Amendola, L. Fabbrizzi, L. Mosca, Anion recognition by hydrogen bonding: urea-based receptors, Chemical Society Reviews 39 (2010) 3889–3915.
[2] K. Lang, J. Park, S. Hong, Urea/transition-metal cooperative catalyst for anti-selective asymmetric nitroaldol reactions, Angewandte Chemie International Edition 51 (7) (2012) 1620–1624.
[3] J.G. Kim, Y. Takami, T. Mizugami, K. Beppu, T. Fukuda, I. Kataoka, CPPU application on size and quality of hardy kiwifruit, Scientia Horticulturae 110 (2006) 219–222.
[4] I. Hayakama, R. Shioya, T. Agatsuma, H. Furokawa, Y. Sugano, Thienopyridine and benzofuran derivatives as potent anti-tumor agents possessing different structure–activity relationship, Bioorganic and Medicinal Chemistry 14 (2004) 3411–3414.
[5] H.R. Heyman, R.R. Frey, P.F. Bousquet, G.A. Cunha, M.D. Moskey, A.A. Ahmed, N.B. Soni, P.A. Marcotte, L.J. Pease, K.B. Glaser, M. Yates, J.J. Bouska, D.H. Albert, C.L. Black Schaefer, P.J. Dandliker, K.D. Stewart, P. Rafferty, S.K. Davidsen, M.R. Michaelides, M.L. Curtin, Thienopyridine urea inhibitors of KDR kinase, Bioorganic and Medicinal Chemistry Letters 17 (2007) 1246–1249.
[6] M.-J.R.P. Queiroz, R.C. Calhelha, L.A. Vale-Silva, E. Pinto, R.T. Lima, M.H. Vasconcelos, Efficient synthesis of 6-(hetero)arylthieno[3,2-*b*]pyridines by Suzuki-Miyaura coupling. Evaluation of growth inhibition in human tumor cell lines, SARs and effects on the cell cycle, European Journal of Medical Chemistry 45 (2010) 5628–5634.
[7] Y. Malam, M. Loizidou, A.M. Seifalian, Liposomes and nanoparticles: nanosized vehicles for drug delivery in cancer, Trends in Pharmacological Sciences 30 (2009) 592–599.
[8] S. Batzri, E.D. Korn, Single bilayer liposomes prepared without sonication, BBA: Biomembranes 298 (1973) 1015–1019.
[9] J.M.H. Kremer, M.W.J.V.D. Esker, C. Pathmamanoharan, P.H. Wiersema, Vesicles of variable diameter prepared by a modified injection method, Biochemistry 16 (1977) 3932–3935.
[10] J.R. Nordlund, C.F. Schmidt, S.N. Dicken, T.E. Thompson, Transbilayer distribution of phosphatidylethanolamine in large and small unilamellar vesicles, Biochemistry 20 (1981) 3237–3241.
[11] B.R. Lentz, Membrane "fluidity" as detected by diphenylhexatriene probes, Chemistry and Physics of Lipids 50 (1989) 171–190.
[12] E. Feitosa, P.C.A. Barreleiro, G. Olofsson, Phase transition in dioctadecyldimethylammonium bromide and chloride vesicles prepared by different methods, Chemistry and Physics of Lipids 105 (2000) 201–213.
[13] J.S. Vincent, S.D. Revak, C.D. Cochrane, I.W. Levin, Interactions of model human pulmonary surfactants with a mixed phospholipid bilayer assembly: Raman spectroscopic studies, Biochemistry 32 (1993) 8228–8238.
[14] J.N. Demas, G.A. Crosby, Measurement of photoluminescence quantum yields – review, Journal of Physical Chemistry 75 (1971) 991–1024.
[15] S. Fery-Forgues, D. Lavabre, Are fluorescence quantum yields so tricky to measure? A demonstration using familiar stationery products, Journal of Chemical Education 76 (1999) 1260–1264.
[16] S.R. Meech, D. Phillips, Photophysics of some common fluorescence standards, Journal of Photochemistry 23 (1983) 193–217.
[17] J.R. Lakowicz, Principles of Fluorescence Spectroscopy, Kluwer Academic/Plenum Press, New York, 1999.
[18] N. Mataga, T. Kubota, Molecular Interactions and Electronic Spectra, Marcel Dekker, New York, 1970.
[19] N.G. Bakhshiev, Universal molecular interactions and their effects on the position of the electronic spectra of molecules in two component solutions. I. Theory (liquid solutions), Optics and Spectroscopy 10 (1961) 379–384.

[20] N.G. Bakhshiev, Universal molecular interactions and their effects on the position of the electronic spectra of molecules in two component solutions, Optics and Spectroscopy 12 (1962) 309–313;
N.G. Bakhshiev, Universal molecular interactions and their effects on the position of the electronic spectra of molecules in two component solutions, Optics and Spectroscopy 13 (1962) 24–29.
[21] M.-J.R.P. Queiroz, S. Dias, D. Peixoto, A.R.O. Rodrigues, A.D.S. Oliveira, P.J.G. Coutinho, L.A. Vale-Silva, E. Pinto, E.M.S. Castanheira, New potential antitumoral di(hetero)arylether derivatives in the thieno[3,2-b]pyridine series: synthesis and fluorescence studies in solution and in nanoliposomes, Journal of Photochemistry and Photobiology A: Chemistry 238 (2012) 71–80.
[22] (a) K.C. James, P.R. Noyce, Hydrogen bonding between testosterone propionate and solvent in chloroform-cyclohexane solutions, Spectrochimica Acta Part A 27 (1971) 691–696;
(b) G.R. Wiley, S.I. Miller, Thermodynamic parameters for hydrogen-bonding of chloroform with Lewis bases in cyclohexane – proton magnetic-resonance study, Journal of the American Chemical Society 94 (1972) 3287–3293.
[23] D.R. Lide (Ed.), Handbook of Chemistry and Physics, 83rd edition, CRC Press, Boca Raton, 2002.
[24] M.J. Frisch, G.W. Trucks, H.B. Schlegel, G.E. Scuseria, M.A. Robb, J.R. Cheeseman, G. Scalmani, V. Barone, B. Mennucci, G.A. Petersson, H. Nakatsuji, M. Caricato, X. Li, H.P. Hratchian, A.F. Izmaylov, J. Bloino, G. Zheng, J.L. Sonnenberg, M. Hada, M. Ehara, K. Toyota, R. Fukuda, J. Hasegawa, M. Ishida, T. Nakajima, Y. Honda, O. Kitao, H. Nakai, T. Vreven, J.A. Montgomery Jr., J.E. Peralta, F. Ogliaro, M. Bearpark, J.J. Heyd, E. Brothers, K.N. Kudin, V.N. Staroverov, R. Kobayashi, J. Normand, K. Raghavachari, A. Rendell, J.C. Burant, S.S. Iyengar, J. Tomasi, M. Cossi, N. Rega, J.M. Millam, M. Klene, J.E. Knox, J.B. Cross, V. Bakken, C. Adamo, J. Jaramillo, R. Gomperts, R.E. Stratmann, O. Yazyev, A.J. Austin, R. Cammi, C. Pomelli, J.W. Ochterski, R.L. Martin, K. Morokuma, V.G. Zakrzewski, G.A. Voth, P. Salvador, J.J. Dannenberg, S. Dapprich, A.D. Daniels, Ö. Farkas, J.B. Foresman, J.V. Ortiz, J. Cioslowski, D.J. Fox, Gaussian 09, Revision A.02, Gaussian Inc., Wallingford, CT, 2009.
[25] (a) T. Yanaia, D.P. Tewb, N.C. Handy, A new hybrid exchange–correlation functional using the Coulomb-attenuating method (CAM-B3LYP), Chemical Physics Letters 393 (2004) 51–57;
(b) M.J.G. Peach, T. Helgaker, P. Sałek, T.W. Keal, O.B. Lutnæs, D.J. Tozer, N.C. Handy, Assessment of a Coulomb-attenuated exchange–correlation energy functional, Physical Chemistry Chemical Physics 8 (2006) 558–562.
[26] C. Toniolo, M. Crisma, F. Formaggio, C. Peggion, V. Monaco, C. Goulard, S. Rebuffat, B. Bodo, Effect of N^{α}-acyl chain length on the membrane-modifying properties of synthetic analogs of the lipopeptaibol trichogin GA IV, Journal of the American Chemical Society 118 (1996) 4952–4958.
[27] M. Crisma, A. Barazza, F. Formaggio, B. Kaptein, B.Q. Broxterman, J. Kamphuis, C. Toniolo, Peptaibolin: synthesis, 3D-structure, and membrane modifying properties of the natural antibiotic and selected analogues, Tetrahedron 57 (2001) 2813–2825.
[28] D. Papahadjopoulos, N. Miller, Phospholipid model membranes. I. Structural characteristics of hydrated liquid crystals, Biochimica et Biophysica Acta 135 (1967) 624–638.
[29] B. Valeur, Molecular Fluorescence – Principles and Applications, Wiley-VCH, Weinheim, 2002.
[30] R.L. Melnick, H.C. Haspel, M. Goldenberg, L.M. Greenbaum, S. Weinstein, Use of fluorescent probes that form intramolecular excimers to monitor structural changes in model and biological membranes, Biophysical Journal 34 (1981) 499–515.
[31] L.M. Almeida, W.L. Vaz, K.A. Zachariasse, V.M. Madeira, Fluidity of sarcoplasmic reticulum membranes investigated with dipyrenylpropane, an intramolecular excimer probe, Biochemistry 21 (1982) 5972–5977.
[32] S. Kang, I.G. Kang, I. Yun, Determination of microviscosity and location of 1,3-di(1-pyrenyl)propane in brain membranes, Archives of Pharmacal Research 20 (1997) 1–6.
[33] E. Szajdzinska-Pietek, M. Wolszczak, A. Plonka, S. Schlick, Fluorescence studies of self-assembling in aqueous solutions of poly(ethylene-*co*-methacrylic acid) (EMAA) ionomers, Journal of the American Chemical Society 120 (1998) 4215–4221.
[34] Y. Díaz-Fernández, S. Rodríguez-Calvo, A. Pérez-Gramatges, P. Pallavicini, S. Patroni, C. Mangano, Effect of surfactant structure on the residual fluorescence of micelle-based fluorescent probes, Journal of Colloid and Interface Science 313 (2007) 638–644.
[35] Y.A. Díaz-Fernández, E. Mottini, L. Pasotti, E.F. Craparo, G. Giammona, G. Cavallaro, P. Pallavicini, Multicomponent polymeric micelles based on polyaspartamide as tunable fluorescent pH-window biosensors, Biosensors and Bioelectronics 26 (2010) 29–35.